Supportting Information

Achieving visible and near-infrared dual-emitting mechanoluminescence in Mn^{2+} single-doped magnesium aluminate spinel

Tianli Wang[a], Fei Liu[a,*], Ziqi Wang[a], Jia Zhang[a], Shuaishuai Yu[a], Junxiao Wu[a], Jiahao Huang[a], Wenjie Wang[c,*], Lei Zhao[b,*]

a. School of Physics and Opto-Electronic Technology, Collaborative Innovation Center of Rare-Earth Optical Functional Materials and Devices Development, Baoji University of Arts and Sciences, Baoji, Shaanxi 721016, P. R. China.

b. Pillar of Engineering Product Development, Singapore University of Technology and Design, 8 Somapah Road, Singapore 487372, Singapore.

c. College of Chemistry and Chemical Engineering, Lanzhou University, Lanzhou, Gansu 730000, P. R. China.

* Corresponding author's E-mail: bwllf@163.com (Fei Liu), wwj@lzu.edu.cn (Wenjie Wang), zhaoleibjwl@163.com (Lei Zhao).

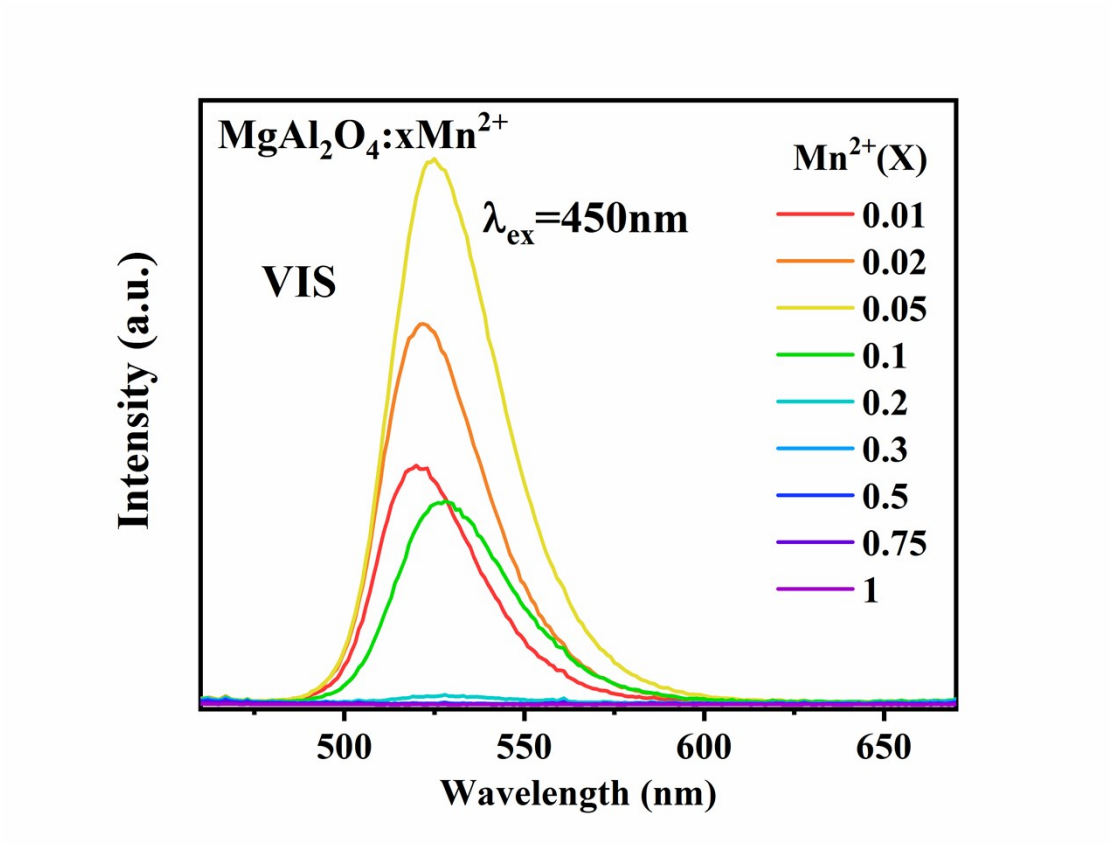

Fig. S1. The Visible PL spectra of $Mg_{1-x}Mn_xAl_2O_4$ (x = 0.01–1.0) upon 450 nm excitation.

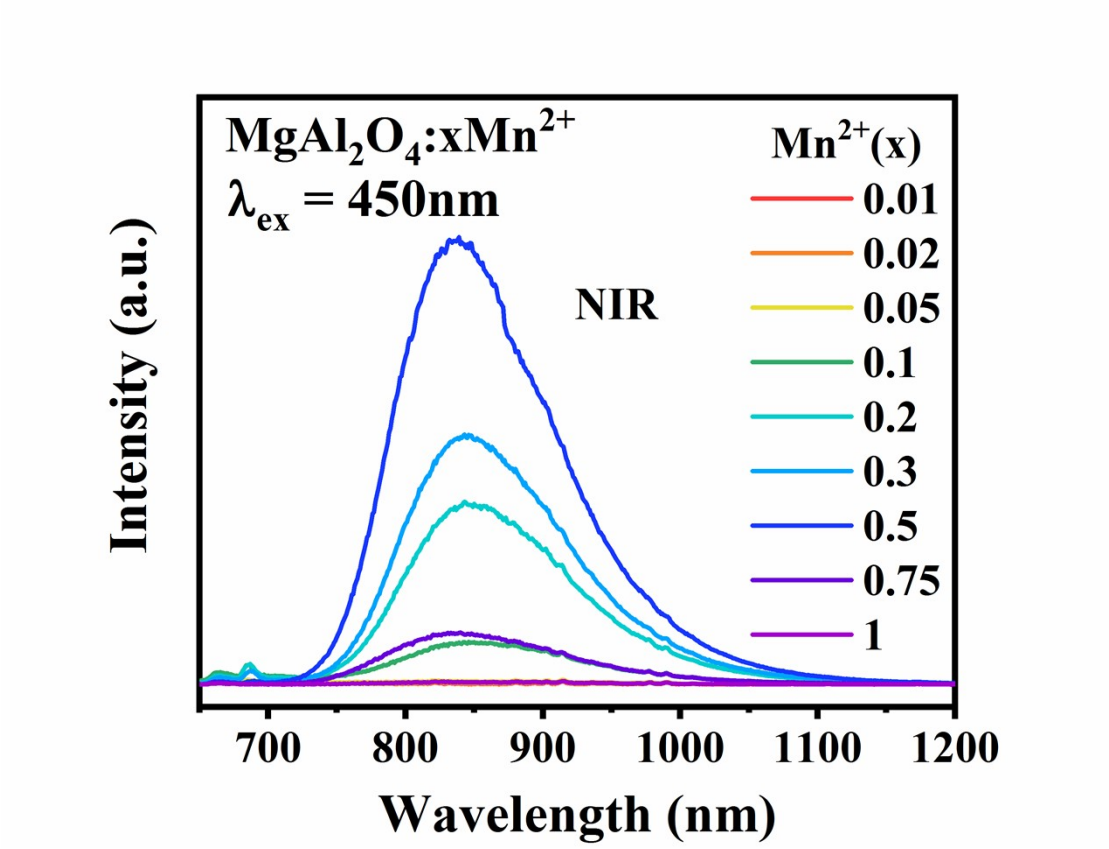

Fig. S2. The NIR PL spectra of $Mg_{1-x}Mn_xAl_2O_4$ (x = 0.01–1.0) upon 450 nm excitation.

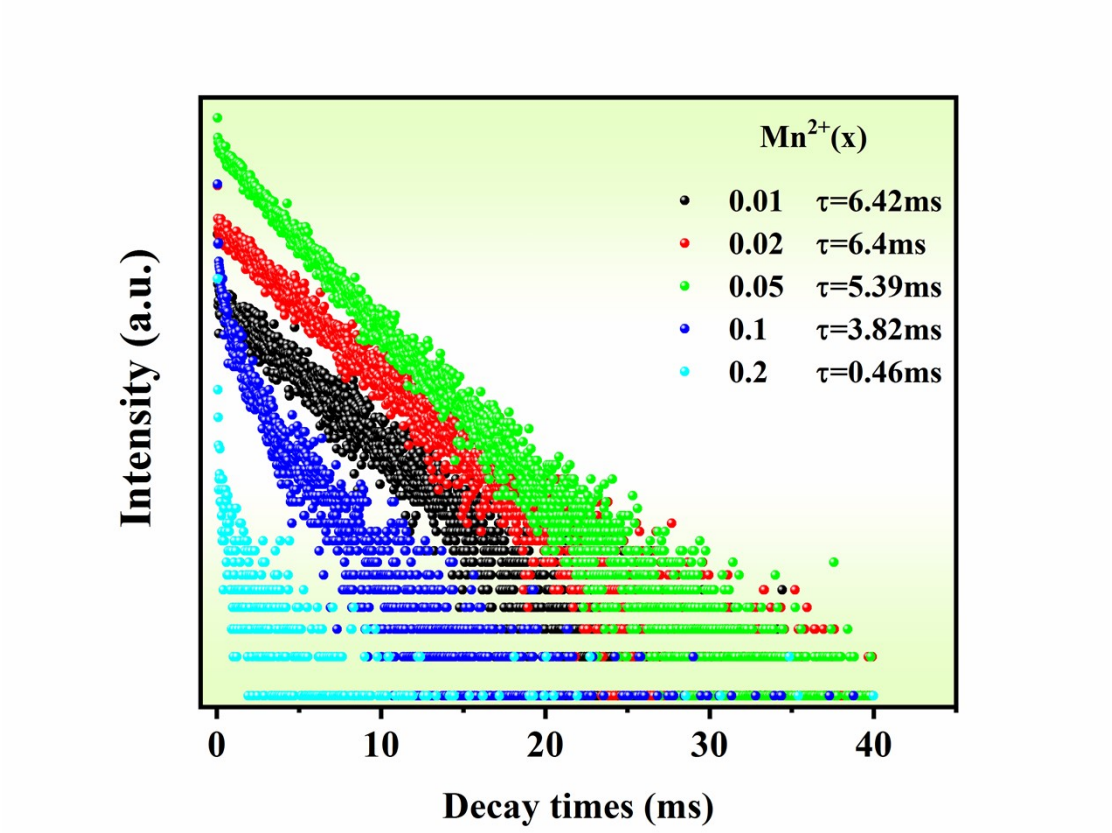

Fig. S3. Luminescence decay curves of $Mg_{1-x}Mn_xAl_2O_4$ (x = 0.01–1.0) (λ_{ex} = 450 nm, λ_{em} = 525 nm).

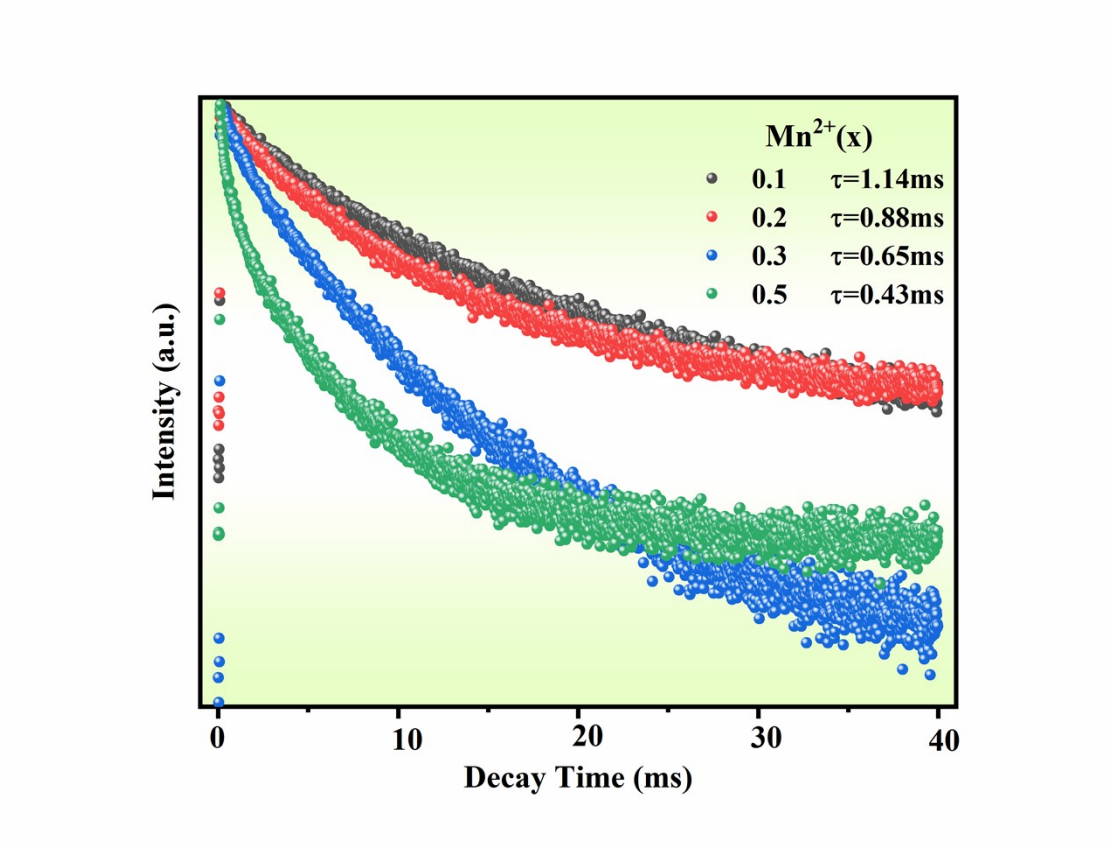

Fig. S4. Luminescence decay curves of $Mg_{1-x}Mn_xAl_2O_4$ (x = 0.1-0.5) (λ_{ex} = 450 nm, λ_{em} = 835 nm).

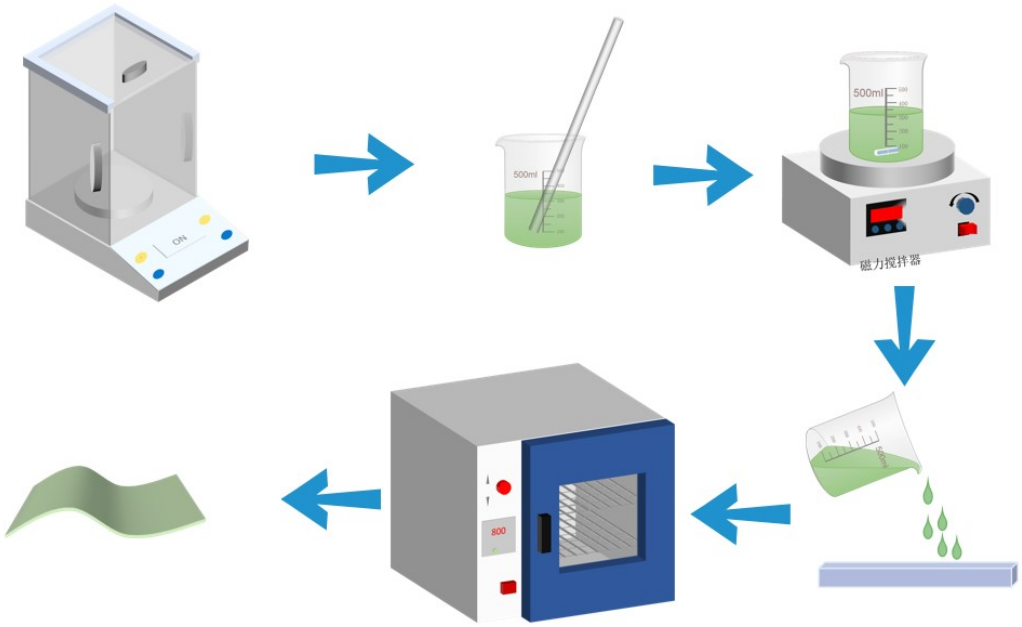

Fig. S5 Schematic diagram of composite device fabrication.

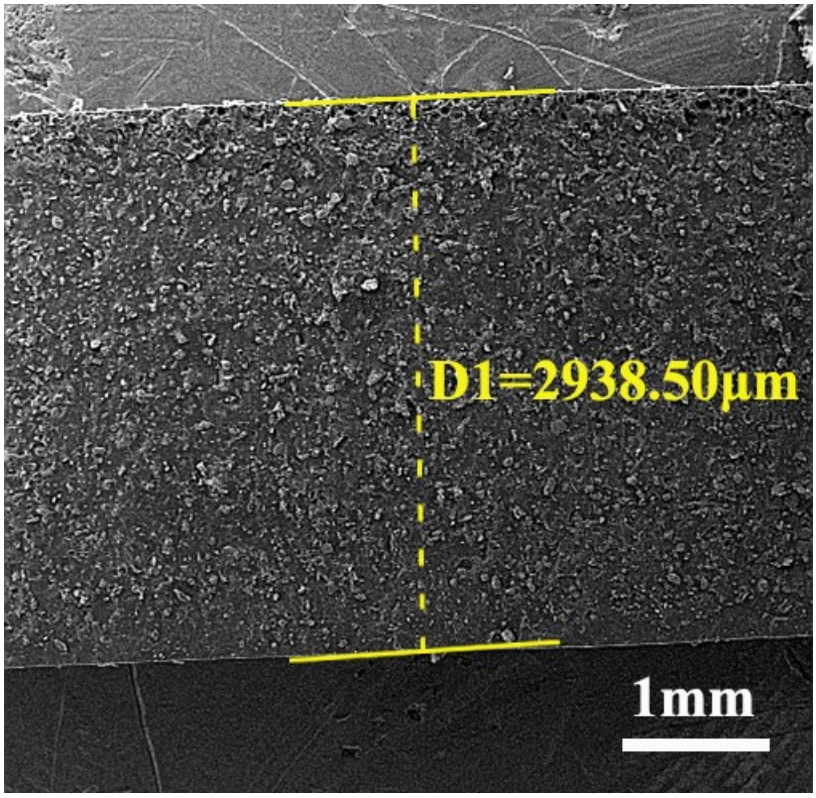

Fig. S6. The SEM images of a cross-section of $MgAl_2O_4$:0.05Mn^{2+}/PDMS films.

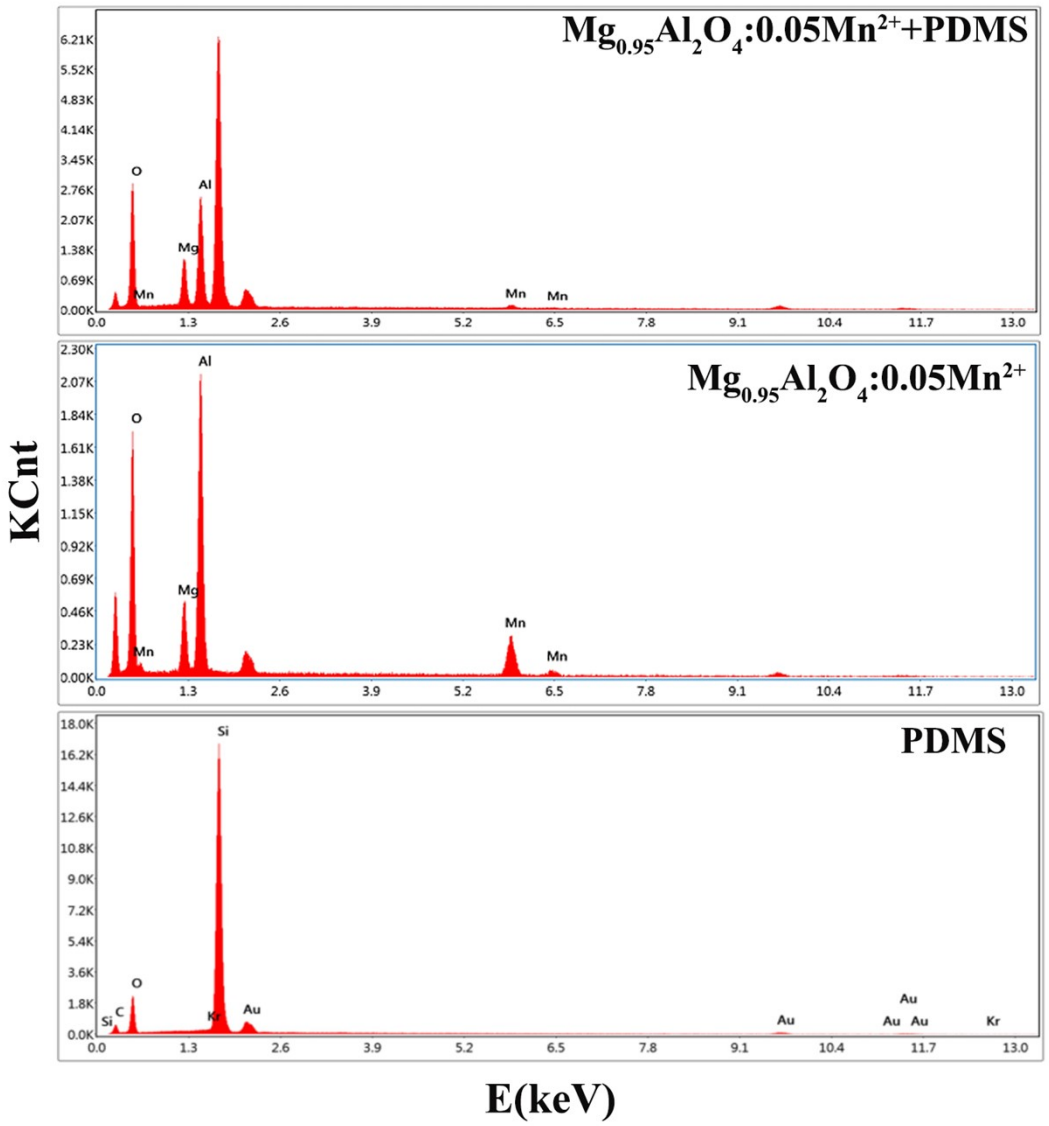

Fig. S7. EDS pattern showing compositional analysis of PDMS, $MgAl_2O_4$:0.05Mn^{2+} and $MgAl_2O_4$:0.05Mn^{2+}/PDMS composite film.

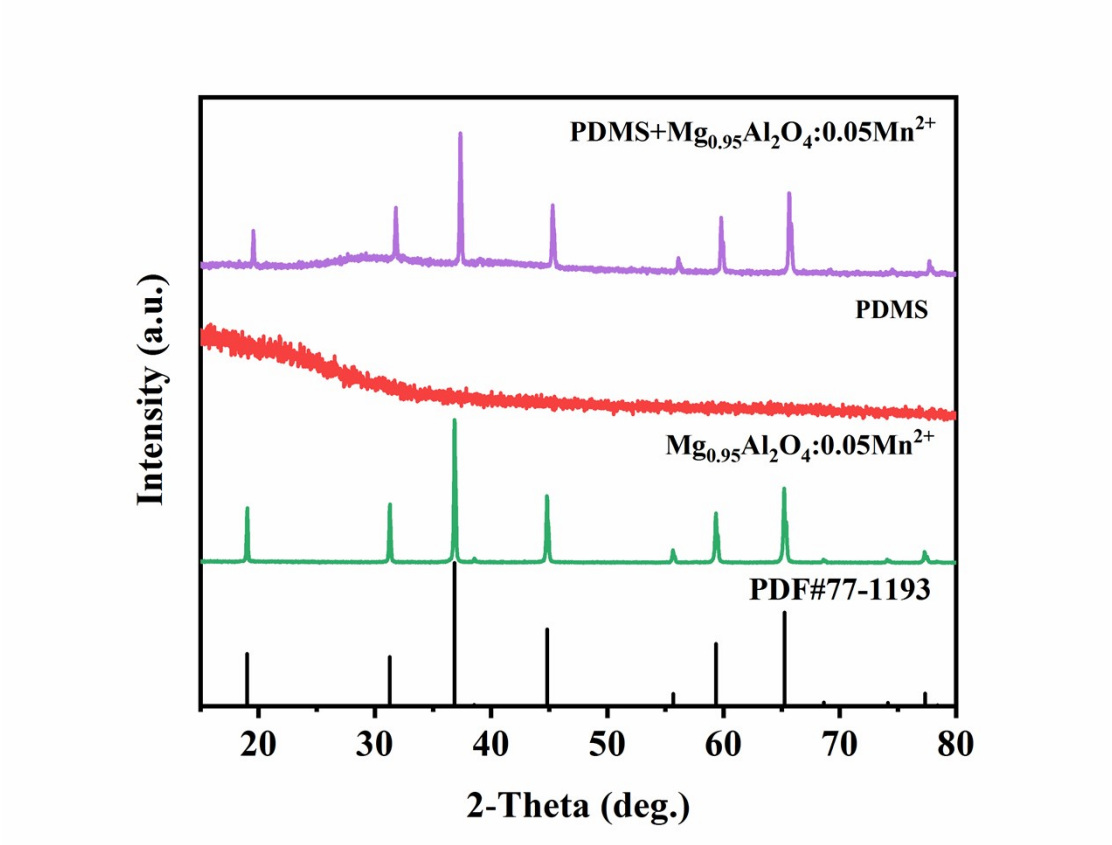

Fig. S8. XRD patterns of as-prepared $MgAl_2O_4$: $0.05Mn^{2+}$ samples and PDMS and thin film and the standard data of the $MgAl_2O_4$ phase (JCPDS #77-1193).

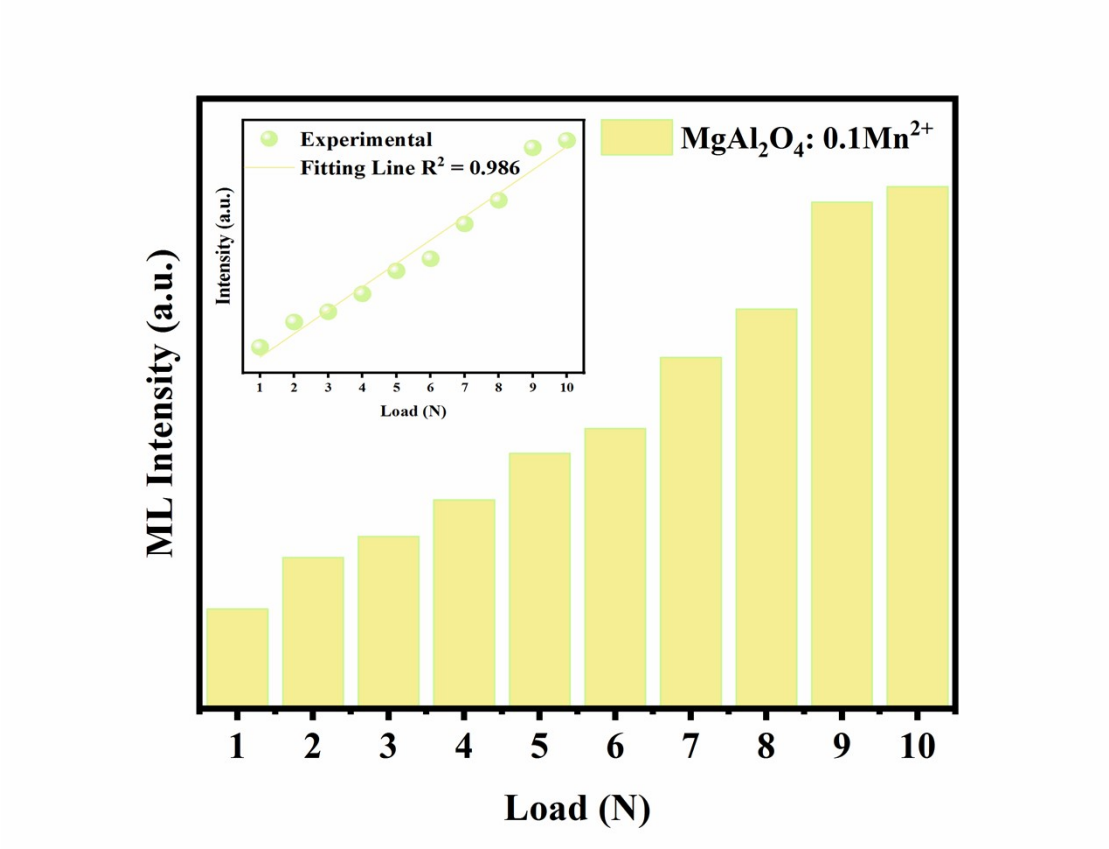

Fig. S9. The mechanical responses results of $Mg_{0.9}Al_2O_4$: $0.1Mn^{2+}$/PDMS, inset showed the linear relationship between the ML intensity and applied load.

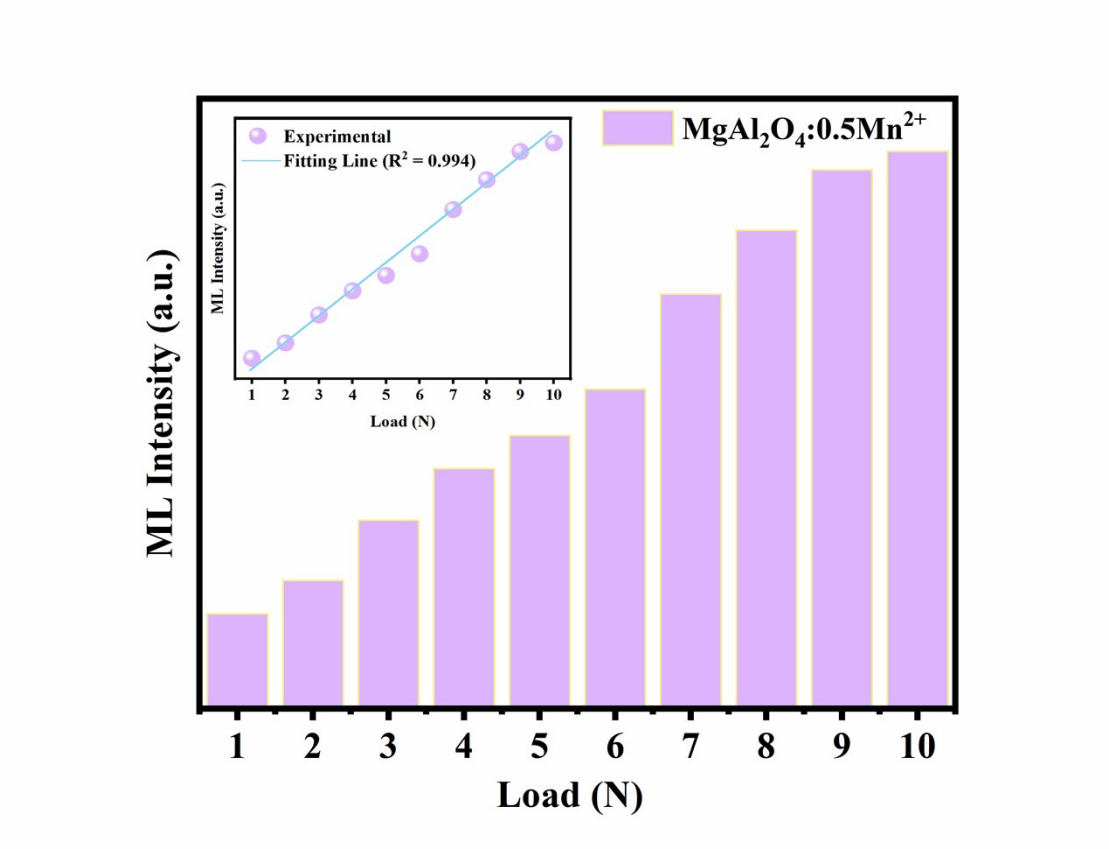

Fig. S10. The mechanical responses results of $Mg_{0.5}Al_2O_4$: $0.5Mn^{2+}$/PDMS, inset showed the linear relationship between the ML intensity and applied load.

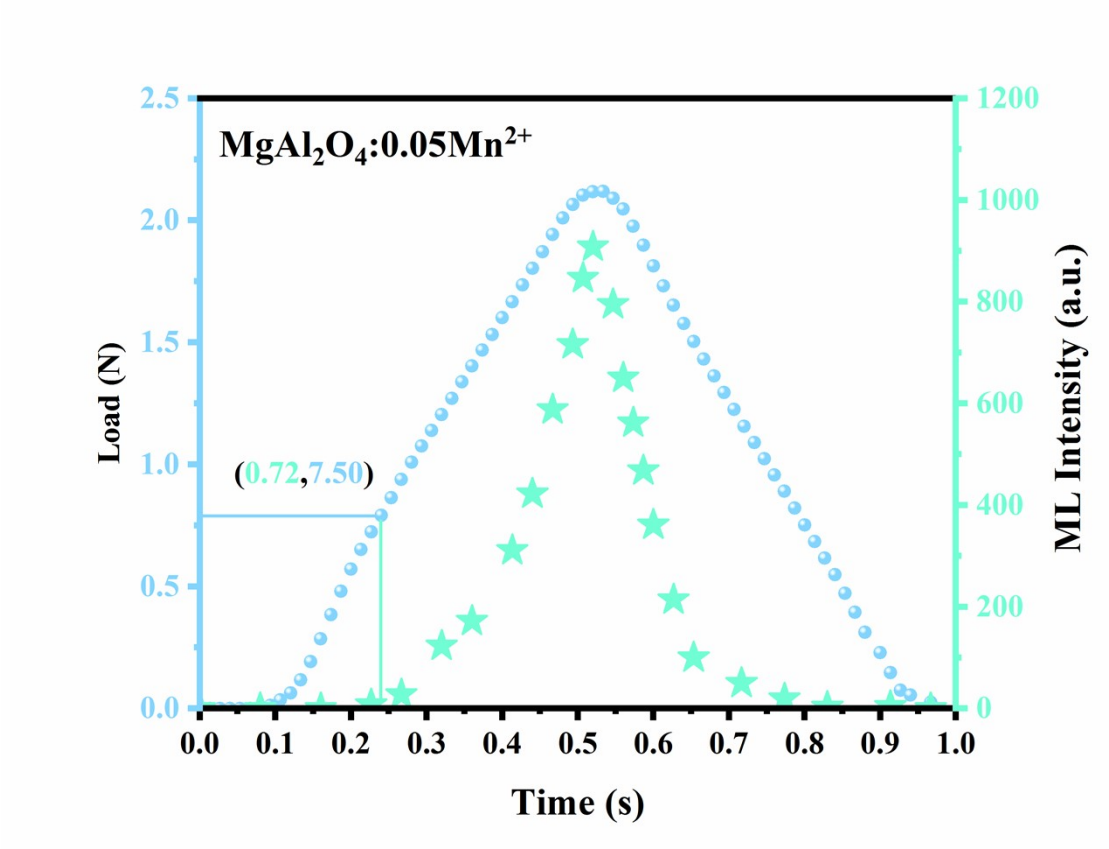

Fig. S11. The relationship between ML intensity and force in the same time of $Mg_{1-x}Al_2O_4$: $0.05Mn^{2+}$/PDMS.

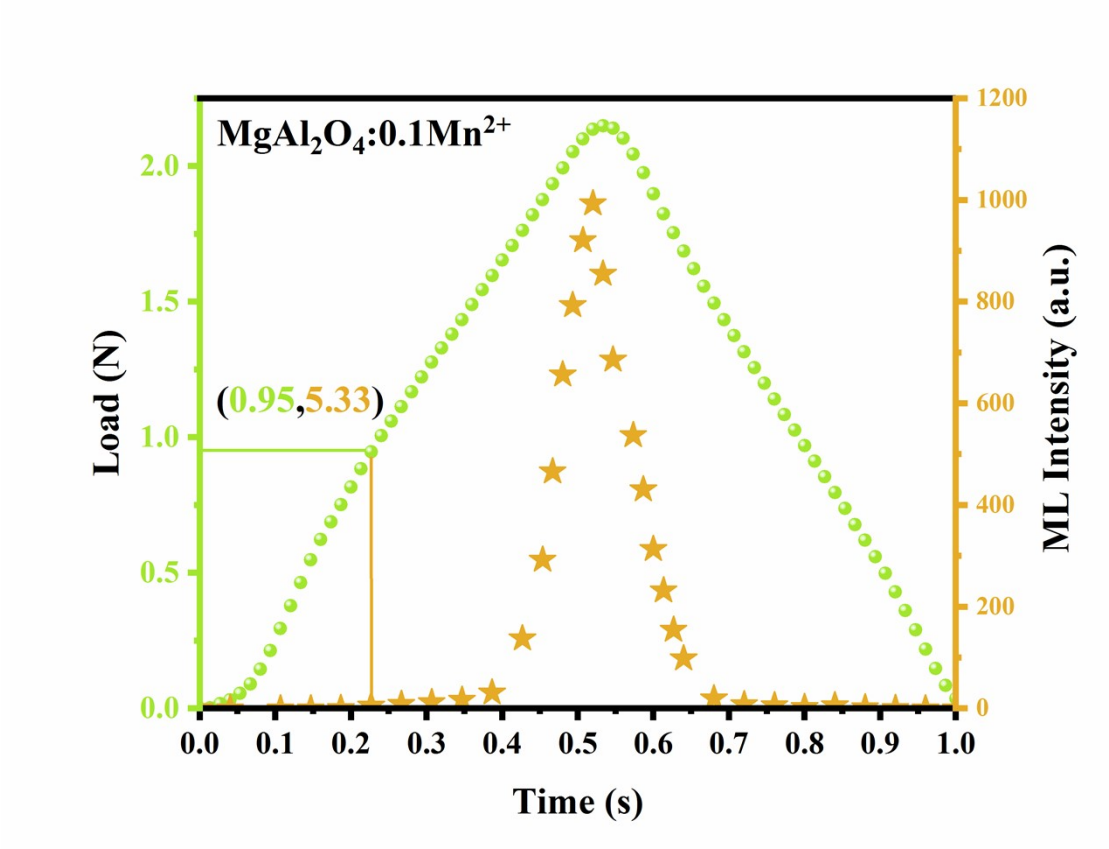

Fig. S12. The relationship between ML intensity and force in the same time of $Mg_{1-x}Al_2O_4$: $0.1Mn^{2+}$/PDMS.

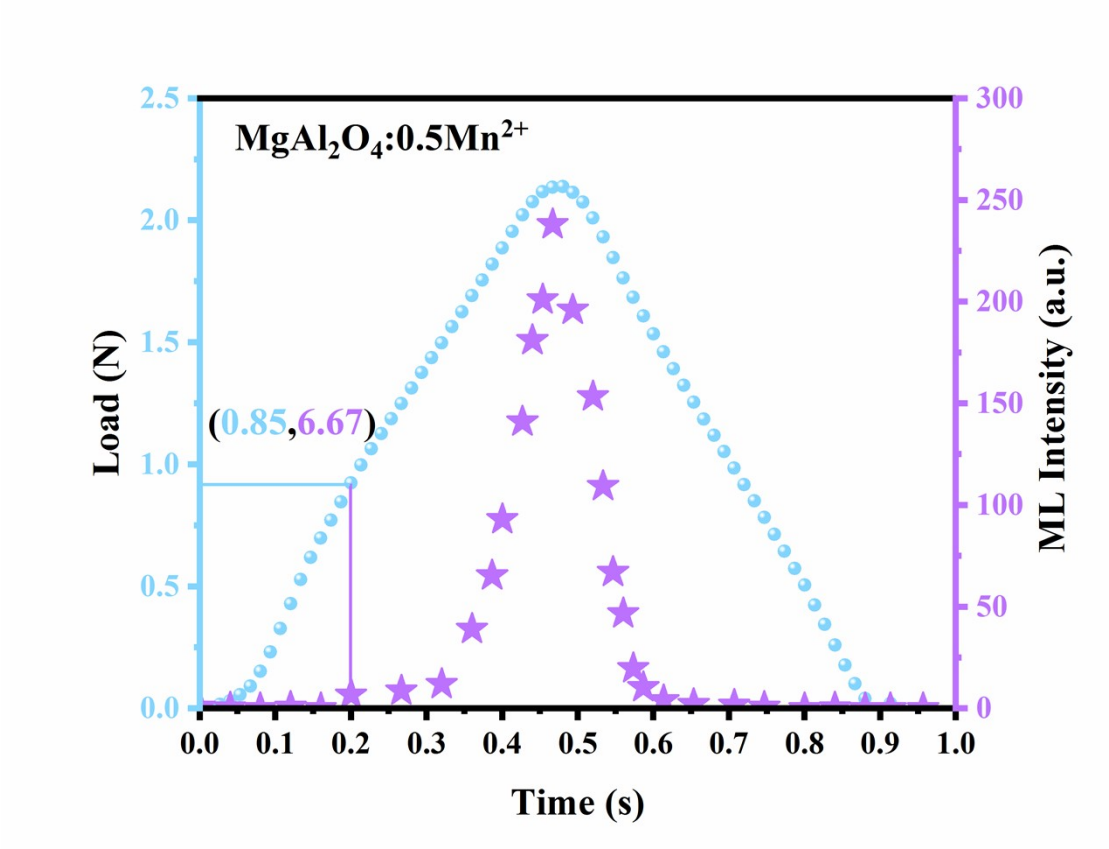

Fig. S13. The relationship between ML intensity and force in the same time of $Mg_{1-x}Al_2O_4$: $0.5Mn^{2+}$/PDMS.

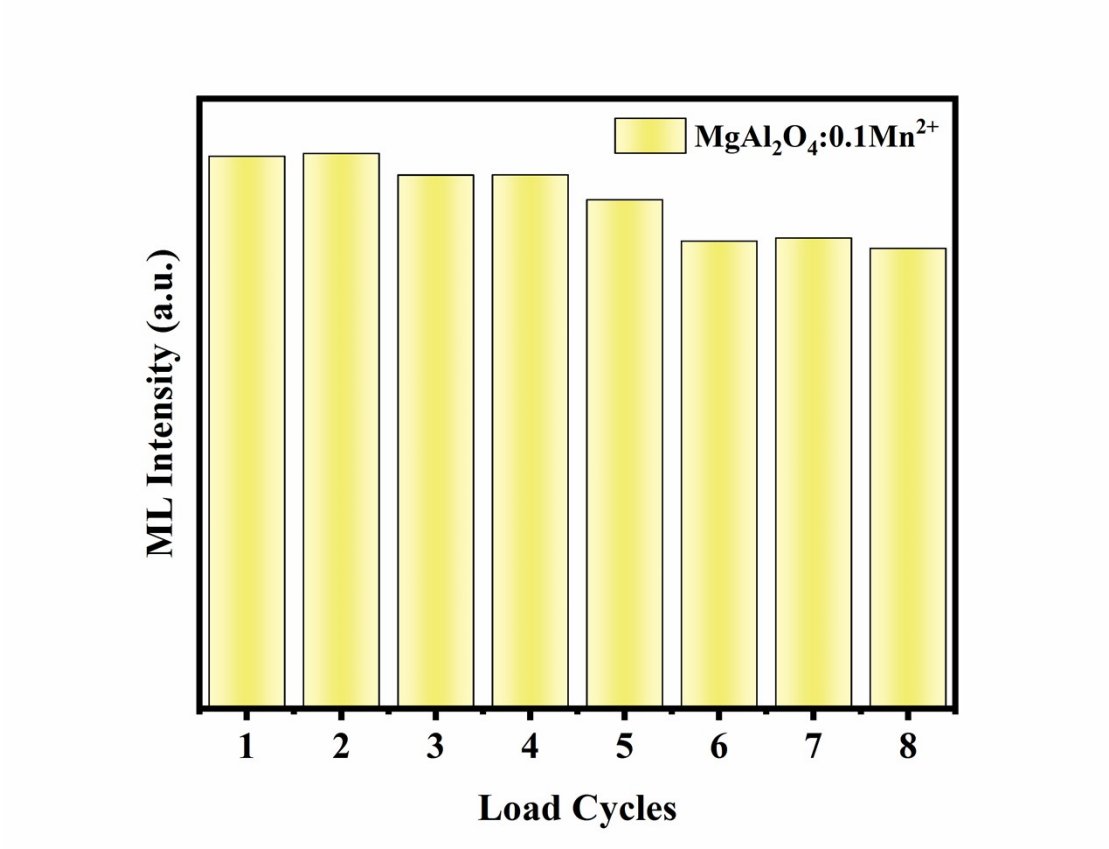

Fig. S14. ML recovery behavior of $Mg_{0.9}Al_2O_4$: $0.1Mn^{2+}$/PDMS under cyclic tests, Max load=2N.

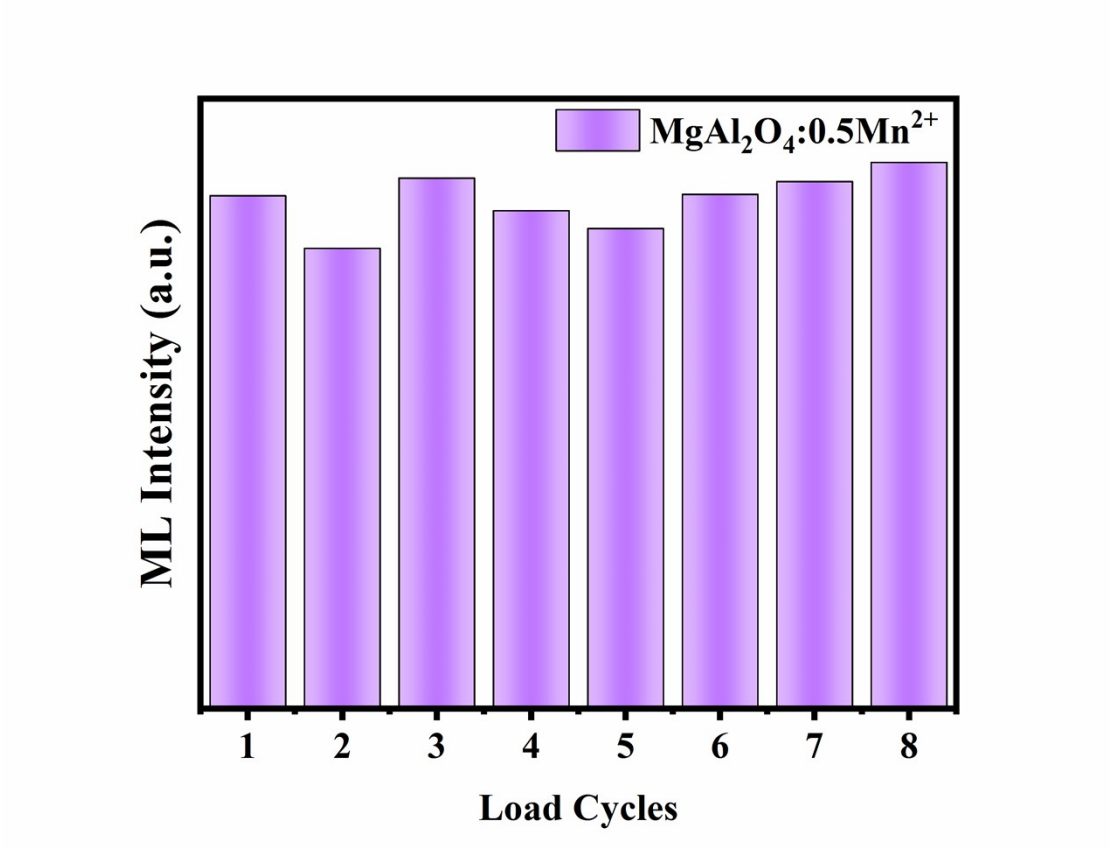

Fig. S15. ML recovery behavior of $Mg_{0.5}Al_2O_4$: $0.5Mn^{2+}$/PDMS under cyclic tests, Max load=2N.

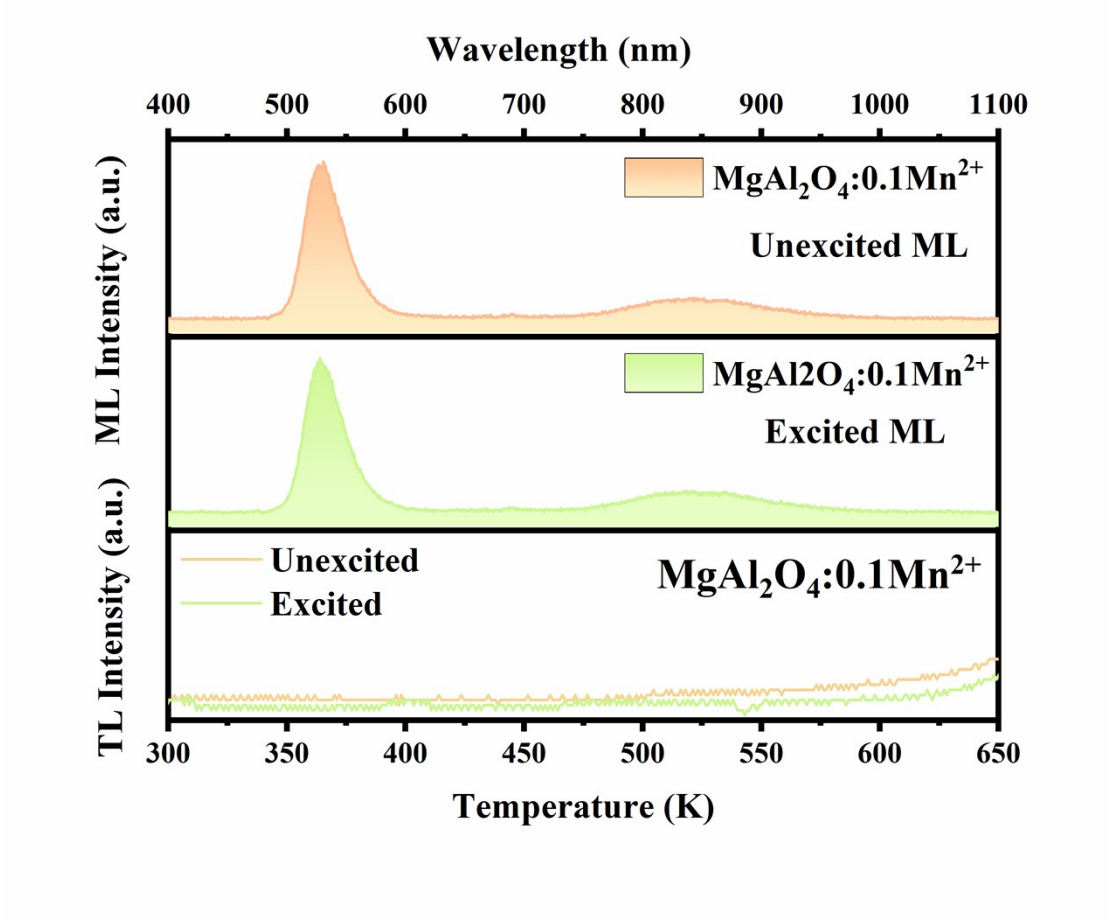

Fig. S16. ML spectra and TL of $Mg_{0.9}Al_2O_4$: $0.1Mn^{2+}$/PDMS by UV light excited and unexcited.

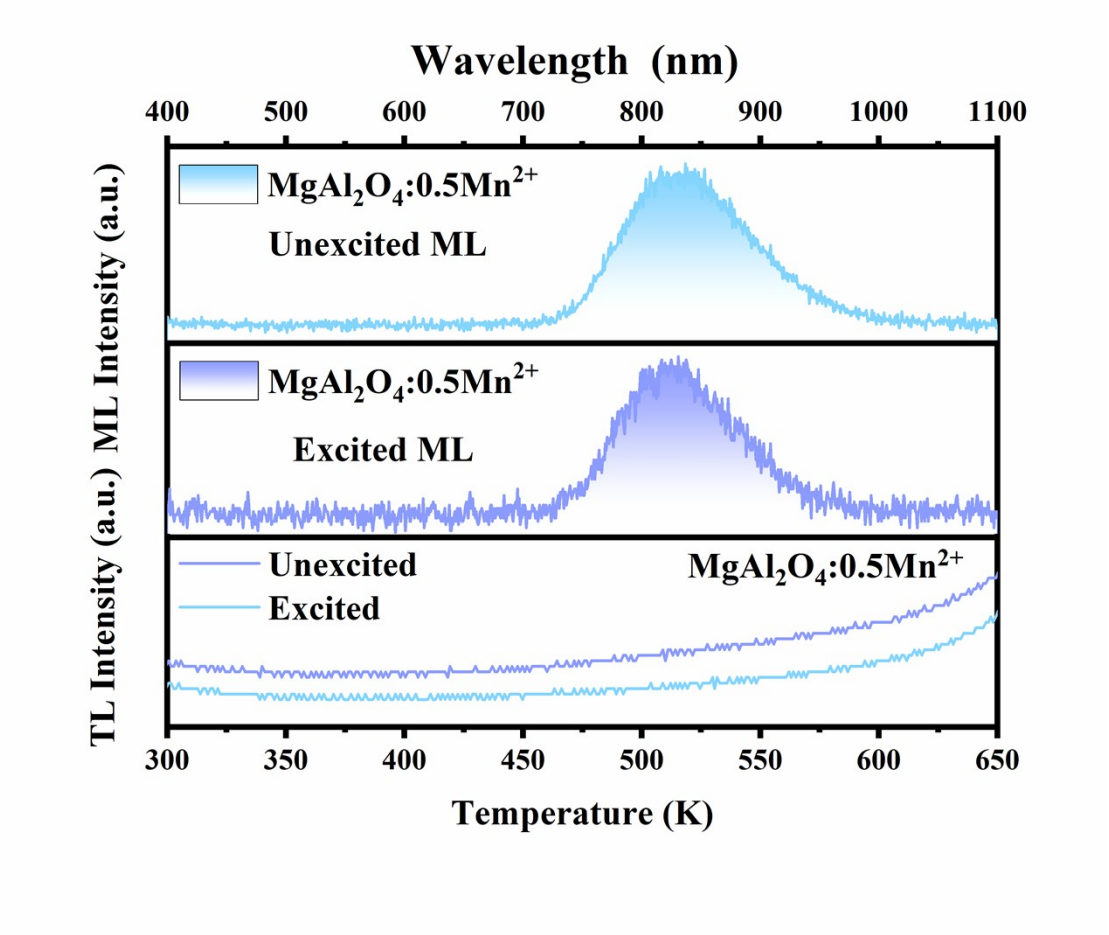

Fig. S17. ML spectra and TL of $Mg_{0.5}Al_2O_4$: $0.5Mn^{2+}$/PDMS by UV light excited and unexcited.